Enhancing daily precipitation reconstruction: An improved version of the `reddPrec` R package

Adrian Huerta[a,b,*], Stefan Brönnimann[a,b], Martín de Luis[c], Santiago Beguería[d], Roberto Serrano-Notivoli[c]

[a] *Institute of Geography, University of Bern, Bern, Switzerland*
[b] *Oeschger Centre for Climate Change Research, Bern, Switzerland*
[c] *Departamento de Geografía y Ordenación del Territorio. Instituto Universitario de Ciencias Ambientales (IUCA), University of Zaragoza, Zaragoza, Spain*
[d] *Estacion Experimental de Aula Dei, Consejo Superior de Investigaciones Científicas (EEAD-CSIC), Zaragoza, Spain*

Abstract

Reconstructing high-quality daily precipitation series is essential for climate studies, hydrological modeling, and environmental applications. This work presents a new version of reddPrec, a versatile and flexible R package designed to reconstruct precipitation datasets through standard quality control, gap-filling, and grid creation procedures. The update introduces greater flexibility in spatial modeling, inclusion of dynamic covariates, and new modules for enhanced quality control and homogenization. Daily precipitation can now be predicted through machine learning approaches within a user-friendly framework, allowing users to select modeling approaches and customize settings. We demonstrate its capabilities through case studies in Switzerland and Spain, evaluating improvements in reconstruction accuracy, quality control, and homogenization. Enhanced quality control and homogenization procedures were specifically validated to ensure reliable adjustment and consistency of precipitation series. Overall, reddPrec provides a comprehensive and reliable tool for reconstructing precipitation series, supporting the creation of high-quality datasets for climate research and related fields.

Keywords: reddPrec, Daily precipitation, Quality control, Missing values, Homogenization, Grid

*Corresponding author
Email address: `adrhuerta@gmail.com` (Adrian Huerta)

1. Introduction

Precipitation data is essential for advancing climate science and supporting a wide range of research and operational applications, including climate modeling, hydrological forecasting, water resource management, ecosystem monitoring, and agriculture. Among the various sources of precipitation measurements, time series recorded by weather stations are considered the most accurate (Tapiador et al., 2012). However, these records often suffer from limitations such as missing values and inhomogeneities, which can compromise their reliability (Venema et al., 2020; Cheng et al., 2024). These challenges are further exacerbated in regions where station networks are sparse or unevenly distributed, often due to economic or geographical constraints (Hunziker et al., 2017, 2018; Bliefernicht et al., 2022). To address these issues, numerous methods have been developed to reconstruct precipitation data, aiming to complete and enhance the quality of observations in both time and space. The resulting reconstructions may take the form of station-level time series (Vicente-Serrano et al., 2010; Tang et al., 2020, 2021; Huerta et al., 2024) or gridded datasets (Serrano-Notivoli et al., 2017a; Aybar et al., 2020; Tang et al., 2022) across a range of spatial and temporal scales. In this context, the `reddPrec` R package (Serrano-Notivoli et al., 2017b) was developed to facilitate the reconstruction of daily precipitation time series.

The `reddPrec` package provides an integrated framework for reconstructing daily precipitation time series from weather station data. It offers a modular function suite that guides users through essential preprocessing steps—including quality control, gap-filling, and grid creation—to ensure that reconstructed datasets are accurate and consistent. Designed with flexibility in mind, `reddPrec` has been successfully applied in regions with dense station networks and moderately complex terrain (Serrano-Notivoli et al., 2017a; Navarro et al., 2020; Škrk et al., 2021; Bessaklia et al., 2021; Centella-Artola et al., 2023; da Silva et al., 2024; Montaño-Caro et al., 2024; Serrano-Notivoli et al., 2024), supporting a wide range of climatological and hydrological studies. However, the original version of the package had several limitations, including a basic quality control protocol, limited support for advanced spatio-temporal models, inflexible handling of dynamic covariates, and the absence of a homogenization tool. These shortcomings limited its effectiveness in more demanding settings, such as areas with sparse station coverage, complex topography, or studies requiring high temporal consistency in the data.

To address the limitations of the original implementation, the new version of reddPrec introduces a suite of methodological improvements aimed at increasing robustness, scalability, and flexibility in the reconstruction process. Key updates include support for user-defined machine learning models in the computation pipeline (Hothorn, 2024), integration of dynamic covariates for spatio-temporal learning (Hu et al., 2019; Ochoa-Rodriguez et al., 2019; Kossieris et al., 2024), an enhanced quality control module for detecting and handling systematic errors in time series input data (Hunziker et al., 2017, 2018), and a homogenization framework (Squintu et al., 2018; Brugnara et al., 2019) tailored for daily precipitation series. These developments enhance the applicability of the package in data-sparse environments and heterogeneous terrain while maintaining compatibility with existing workflows for quality control, gap filling, and grid creation.

This paper presents the updated version of `reddPrec`, detailing its new features and demonstrating their functionality through real-case experiments. Section 1 briefly describes the technical basis and core functions of reddPrec. Section 2 describes the major improvements in the package, focusing on the expanded modeling capabilities, enhanced quality control routines, and the integration of a homogenization framework. Section 3 presents application experiments that showcase the package's performance and impact in reconstructing precipitation. Finally, we discuss potential applications and future developments for further extending the utility of `reddPrec` in climate and hydrological research.

2. Overview of the reddPrec package

The `reddPrec` package is built around the concept of reference values (RVs), which are local precipitation estimates generated for each day and location. These values are derived from nearby weather stations, incorporating topographical covariates to capture the spatial and temporal variability of precipitation. Essentially, RVs provide highly flexible, localized models that reflect the precipitation conditions specific to each station and its surroundings.

RVs are computed through a combination of classification and regression functions. Let $\mathbf{X} = [x_1, x_2, \ldots, x_N]$ represent the vector of covariates, where N denotes the number of covariates, and the process is structured as follows:

1. Classification function: This function classifies each day as either dry or wet based on predicted probabilities:

$$Y_{\text{class}}(\mathbf{X}) = \begin{cases} 1 & \text{if } f_c(\mathbf{X}) + \varepsilon_c \geq 0.5 \\ 0 & \text{if } f_c(\mathbf{X}) + \varepsilon_c < 0.5 \end{cases} \quad (1)$$

   Where $f_c(\mathbf{X}) \in [0, 1]$ is the predicted probability of a wet day, and ε_c is the classification model error.

2. Regression function: This function estimates the amount of precipitation for a given day:

$$Y_{\text{reg}}(\mathbf{X}) = f_r(\mathbf{X}) + \varepsilon_r \quad (2)$$

   Where $f_r(\mathbf{X}) \in \mathbb{R}_{\geq 0}$ is the predicted precipitation amount, and ε_r is the regression error term.

3. RV: The final precipitation estimate is obtained by combining the dry/wet classification and the regression output:

$$RV(\mathbf{X}) = Y_{\text{class}}(\mathbf{X}) \cdot Y_{\text{reg}}(\mathbf{X}) \quad (3)$$

In the original version of reddPrec, RVs were constructed using data from 10 nearby stations, with $N = 3$ covariates (latitude, longitude, and elevation). Both the classification (f_c) and regression (f_r) models were based on generalized linear models (glm).

Once RVs are generated, they are utilized in the core functions of the package to:

1. Apply quality control to raw data using the `qcPrec()` function.
2. Fill missing values in time series through the `gapFilling()` function.
3. Create gridded precipitation datasets using the `gridPcp()` function, where each grid point is treated as an individual station.

3. Updates and new features

The latest version of reddPrec includes various additions aimed at increasing model flexibility and the use of dynamic covariates in core functions. It also provides new functions on quality control and homogenization of precipitation time series. The updates are outlined below.

3.1. Flexibility on model foundation and dynamic covariates on RVs

A key parameter in the computation of RVs is the choice of the statistical model. While the previous version of reddPrec employed glm by default, this approach proved effective primarily in dense station networks and moderately challenging topographies. In regions characterized by sparse station coverage or complex terrain, the glm approach may lead to suboptimal reconstructions (Serrano-Notivoli and Tejedor, 2021).

To address this limitation, the updated version introduces a flexible modeling framework through the new `model_fun` argument, which allows users to specify a custom machine learning model for RV computation. This enhancement broadens the applicability of reddPrec to diverse climatic and geographic contexts by enabling a wide array of classification and regression models available in the R ecosystem. While the original glm-based method remains accessible via `learner_glm()`, the package now includes additional built-in options such as support vector machines (`learner_svm()`), random forests (`learner_rf()`), extreme gradient boosting (`learner_xgboost()`), and neural networks (`learner_nn()`). Users can also define their own models by following the established structure of these learner functions and tailoring the modeling parameters to their specific data and objectives.

In addition to expanding modeling flexibility, the new version of reddPrec introduces support for dynamic covariates (predictors that change their values each time step) in RVs construction through the `dynam_cov` argument. Previously, the package supported only static covariates, limiting its adaptability to real-time or temporally varying predictors. The new implementation allows the incorporation of dynamic variables, such as radar and satellite-based products, or outputs from atmospheric models, which can vary over time. When used alongside static covariates, these dynamic inputs may enable more context-sensitive and accurate reconstructions, particularly in environments where precipitation processes are influenced by rapidly changing atmospheric conditions and with scarce observed data.

3.2. Enhanced quality control

Accurate precipitation reconstruction requires input data to be free from significant errors, inconsistencies, or outliers. In the previous version of reddPrec, quality control was limited to standard spatial-based routines on RVs, which primarily focused on detecting isolated suspicious values. The updated version, however, significantly complements this aspect by introducing a comprehensive and modular quality control system, called enhanced quality control.

The enhanced quality control approach addresses recurring data quality issues that may go undetected by standard methods. Originally developed by Hunziker et al. (2017, 2018), this technique comprises visual tests designed to allow users to remove or flag problematic periods in a time series. In the new reddPrec, these tests have been automated by introducing a classification scheme that evaluates the overall quality of each station. Rather than flagging isolated time series periods, stations are categorized according to their test levels. The enhanced quality control tests include:

- Truncation: Truncation is identified when heavy precipitation episodes are systematically reduced in frequency above a certain threshold. Here, the maximum boundary of a time series is determined as the daily precipitation's maximum moving window value. This boundary is then assessed based on its persistence over time:
    - Level 0: No truncation is detected (the maximum boundary persists for less than 3 years).
    - Level 1: A constant maximum boundary lasts between 3 and 5 years.
    - Level 2: The maximum boundary persists for more than 5 years.

- Small gaps: Small gaps refer to periods of unreported precipitation events that result in a reduction of frequency in low precipitation ranges. For this test, the total counts of precipitation values are computed in five ranges (0–1, 1–2, 2–3, 3–4, and 4–5 mm) for each year. The percentage of years with zero counts in these ranges is used to define the quality level:
  - Level 0: No small gaps (0%; years show at least one value in any range).
  - Level 1: Small gaps persist in at least 20% of consecutive years.
  - Level 2: Small gaps extend for more than 20% of consecutive years.
- Weekly cycle: The weekly cycle examines the occurrence of wet days to detect significant differences between days of the week. For each day, the probability of precipitation is computed by dividing the number of wet days by the total count of records. A two-sided binomial test (using a 95% confidence level) then determines which days show significantly different probabilities:
  - Level 0: No atypical weekly cycle (similar precipitation probabilities across the week).
  - Level 1: At least two days present an atypical probability.
  - Level 2: More than two days show atypical probabilities, or one day exhibits an extremely different probability (a difference of more than 10%).
- Precision and rounding patterns: This test assesses the consistency in decimal precision across the time series. First, the unique decimal patterns (sorted in descending order) are computed for each year. The mode, representing the most dominant decimal pattern, is then identified, and the proportion of the time series displaying this pattern is calculated:
  - Level 0: The dominant decimal pattern is present in more than 70% of the time series, indicating coherent precision.
  - Level 1: The dominant pattern is observed in between 50% and 70% of the data.
  - Level 2: There is no dominant decimal pattern, suggesting inconsistencies in reporting precision.

To improve reproducibility and transparency, these enhanced quality control procedures can be applied automatically using the `eqc_Ts()` function, which computes the quality levels as defined above. However, the thresholds and criteria can be customized based on user needs. In addition, summary plots for visual inspection can be generated with the `eqc_Plot()` function, offering an intuitive overview of the quality classification for each station as it was originally established in Hunziker et al. (2017, 2018).

By incorporating these robust quality control checks into the core functions of reddPrec, the updated package can ensure that reliable and consistent data are used in both the construction of RVs and the final precipitation estimates, thereby significantly enhancing the overall robustness and reproducibility of precipitation reconstructions.

3.3. Homogenization

Inhomogeneities (e.g., changes in station location, instrumentation, and observation techniques) in precipitation time series can significantly affect statistical reconstructions and climatological analyses. To address this issue, the new version of reddPrec incorporates a homogenization framework specifically designed for daily precipitation datasets.

This procedure builds upon methods previously applied at global and continental scales (Squintu et al., 2018; Brugnara et al., 2019), with targeted adaptations for daily precipitation. It combines the strengths of both relative and absolute approaches. Relative homogenization uses comparison between stations, while absolute homogenization uses individual station data to detect/adjust changes. Although absolute methods generally have lower detection power than relative ones (Venema et al., 2012), they serve as a critical fallback when relative testing is not feasible (such as in scarce-station networks). The entire procedure is implemented in the `hmgTs()` function and follows three main stages:

- Break detection: A combination of statistical tests and intercomparison of their results is used to detect breakpoints. Five univariate breakpoint tests are applied: Student's t-test, Mann-Whitney, Buishand R, Pettitt, and the Standard Normal Homogeneity Test. In the relative approach, the algorithm identifies up to `neibs_max` well-correlated stations (correlation > `cor_neibs`) within a specified radius distance (`thres`). These nearby stations are used to construct difference series (target minus neighbor) under three temporal aggregations (annual, April–September, and October–March) and two indices (PRCPTOT: total precipitation; R1mm: number of wet days). A breakpoint is confirmed in a given year if it is detected in at least `perc_break` percent of the significant difference series (p-value $<$ 0.05), with a tolerance of ± 1 year. If fewer than `neibs_min` nearby stations are found, the algorithm defaults to the absolute approach.

- Adjustment: A quantile-matching technique is used to adjust detected breaks, following the methodology of Squintu et al. (2018). While originally developed for temperature data, the method has been adapted here for precipitation. Dry values (i.e., when `wet_day = 0`) are excluded from correction.

Wet values are transformed using both square root and logarithmic functions to approximate a normal distribution before adjustment. In the relative approach, adjustment factors are computed from both the target and nearby series, assuming the post-break period is correct and applying corrections retrospectively. In the absolute case, adjustments rely solely on the target series and function similarly to a quantile mapping procedure.

- Quality control of adjustments: Because daily precipitation adjustments can influence the extreme tails of the distribution, corrected values can be constrained to not exceed a specified threshold difference (controlled via `apply_qc`) compared to the original data. This constraint can be applied either to all values or to values above a defined precipitation threshold (`mm_apply_qc`). This step preserves the correction of extremes while preventing the generation of implausibly large values.

The homogenization workflow is fully integrated into the reddPrec ecosystem and operates seamlessly alongside the quality control and gap-filling modules. It is important to note that `hmgTs()` requires gap-filled input data and is mainly designed to correct inhomogeneities in the gap-filled data. The primary outputs are the homogenized time series and the corresponding break year information. By incorporating homogenization as a core module, the updated reddPrec ensures temporal consistency in the input data, leading to more robust and reliable precipitation reconstructions.

4. Demonstration experiments

The following examples illustrate the performance and practical utility of the newly introduced features in the updated version of reddPrec. Each experiment showcases a specific enhancement and demonstrates its impact on daily precipitation reconstruction.

The primary dataset used for these experiments is the Swiss National Basic Climatological Network (Swiss NBCN), which provides some of the highest-quality and longest continuous precipitation records available (Begert, 2007; Füllemann et al., 2011). Its comprehensive spatial coverage, spanning a range of elevations and climate zones across Switzerland, makes it an ideal testbed for evaluating the methodological improvements. Additional datasets were also used in specific cases, as described in the respective experiment subsections.

4.1. Gap-filling and grid creation

This experiment tested the original reddPrec approach (glm) with two newly integrated model options (rf and xgboost) for gap-filling and grid creation. To facilitate evaluation, we used two complementary metrics: the Matthews correlation coefficient (mcc) and the refined index of agreement (dr). The mcc quantifies performance in dry/wet day classification, while dr assesses the accuracy of wet-day precipitation amounts (Chicco and Jurman, 2023; Willmott et al., 2012). These metrics together enable a comprehensive assessment of both categorical and continuous components of precipitation modeling. The mcc and dr range from -1 (no agreement) to +1 (perfect agreement), with 0 indicating no better than random classification and no predictive skill, respectively (Appendix A).

For the gap-filling task, models were trained using 15 nearby stations with seven static covariates (latitude, longitude, elevation, and the first four principal components of multiple topographic features) over the period 2010–2015. Figure 1 presents leave-one-out cross-validation results in terms of mcc and dr. Both rf and xgboost outperformed glm in overall performance, with the most notable improvements observed in the classification component. Specifically, mcc values showed an average increase of approximately 0.05, with most results clustered at 0.7 and 0.85. In contrast, improvements in dr were more modest (slightly below 0.05), and dispersion remained similar across models. Among the machine learning methods, rf exhibited better efficiency in this setting.

We then applied the same modeling approaches to grid creation. Unlike gap-filling, which estimates missing values at known station locations, grid creation generates precipitation values at ungauged points, treating each grid cell as a virtual station. In this experiment, we produced daily grids at 0.009° resolution ($\approx$ 1 km) over Switzerland for an extreme precipitation event that occurred between July 24–28, 2014. The same set of static covariates was used, with two dynamic covariates added (Figure C.9): MODIS Aqua/Terra surface reflectance bands 1 and 2 (Vermote and Wolfe, 2021). Model outputs were evaluated against the RhydchprobD product (Frei and Isotta, 2019), comparing spatial patterns and point-to-grid values. RhydchprobD, constructed through conditional simulation based on Gaussian Random Fields, served as a robust benchmark due to its use of approximately ten times more observation stations, including those from neighboring countries.

Figures 2 and 3 show the modeled spatial fields and scatterplots of predicted versus observed values at the nearest station-grid point. A visual inspection suggested that all models captured spatial variability well compared to RhydchprobD. Wet to dry areas were realistically distributed, particularly on July 24 (north to south) and July 27 (southwest to northeast). The models also captured high rainfall magnitudes on July 26 (northeast area) and July 28 (southwest area), albeit with lower intensity than RhydchprobD. While spatial patterns were similar across models, rf and xgboost better preserved observed values than glm (Figure 3). The mcc and dr values were consistently close to 1 for both rf and xgboost. In contrast, the glm exhibited some days with values near 0.5, reflecting lower accuracy. These results demonstrate that rf and xgboost provide improved modeling of both wet/dry day classification and wet-day precipitation amounts. The lower extremes of magnitude and slightly reduced coherence in our model outputs, compared to RhydchprobD, likely result from using fewer input stations. Nonetheless, this highlights the robustness of reddPrec under limited data scenarios and complex terrain.

To further test the flexibility of the grid-creation workflow, we applied the same approaches to an extreme rainfall event in eastern Spain. This case focuses on the torrential rainfall that occurred in the province of Valencia on October 29, 2024, which led to widespread flooding and infrastructure disruption. Unlike the Swiss case, the Spanish station network was denser but unevenly distributed, offering a realistic test of modeling under operational constraints (Figure C.10). Daily precipitation data from 443 AEMET (and other sources) stations were used to generate 0.009° ($\approx$ 1 km) grids over the affected region. The same dynamic covariates were included, alongside three static covariates (latitude, longitude, elevation). Model outputs were compared against a reference grid produced by the Consejo Superior de Investigaciones Científicas (CSIC), which used the same station data (Beguería et al., 2024) through a universal kriging approach using (rescaled) coordinates and elevation as covariates.

Figure 4 shows the spatial precipitation fields and the predicted vs. observed scatterplots for each model and the CSIC reference. Visually (Figure 4a), all models reproduced the spatial structure and localized intensity of the event, capturing accumulations up to 700–800 mm (maximum 24h precipitation recorded was 772 mm (AEMET, 2024)). In terms of value preservation (Figure 4b), all models performed well (mcc and dr near 1), though rf and xgboost once again achieved tighter fits (i.e., less spread). The CSIC product showed a nearly perfect match, likely due to its modeling technique (nugget effect), which aims to replicate exact station values.

These experiments highlight the versatility and strength of reddPrec in handling both gap-filling and grid creation tasks across diverse geographic and data scenarios. By integrating advanced machine learning techniques and dynamic covariates, the package can deliver accurate reconstructions even under diverse conditions, such as dense to sparse or uneven station networks and high-intensity precipitation events. While default model configurations already yield solid results, performance can be improved through hyperparameter optimization, tailored covariate selection, and domain-specific user input. Overall, reddPrec offers a flexible and scalable precipitation modeling framework, supporting research applications and operational needs in climate and hydrological monitoring.

4.2. Enhanced quality control

To ensure the reliability of precipitation series before modeling or reconstruction, reddPrec introduces an enhanced quality control (QC) framework. This feature extends the standard QC procedures by incorporating both visual and automatic diagnostic tools to detect subtle or non-obvious data issues.

We first illustrate the functionality of the enhanced QC with `eqc_Plot()`, which provides an integrated diagnostic overview for individual time series. Figure 5 shows an example output from this function for two contrasting stations: one with high-quality data and another exhibiting significant quality deficiencies. Each panel includes time series plots of the full precipitation range, along with a focused view of low precipitation values (0 to 5 mm) to highlight anomalies in the light-rain regime. In addition, four key diagnostic components support the enhanced QC checks:

- Truncation: A smoothed line plot highlights periods dominated by constant heavy precipitation values, which may indicate sensor or recording issues. This commonly occurs when rain gauges are not emptied promptly, causing overflow and truncation of extreme events. Such censoring can lead to underestimation of total rainfall during intense events and may distort analyses of extremes, including intensity-duration-frequency curves, risk assessments, and infrastructure planning (e.g., flood defenses).

- Small gaps: A set of colored lines displays the yearly counts of precipitation values within sub-millimeter intervals (e.g., 0–1 mm, 1–2 mm, etc., excluding integers), helping to detect systematic omissions of light precipitation. These gaps may arise from observer errors (missed or rounded records), instrument limitations (e.g., tipping buckets failing to register drizzle), or processing steps (e.g., aggregation or flagging). Such omissions bias rainfall statistics by underestimating light precipitation frequency and totals, ultimately affecting wet-day counts, rainfall intensity distributions, and climate trend analyses.

- Weekly cycle: A bar plot shows the fraction of wet days for each day of the week, with annotations above each bar indicating the count of wet days and a dotted line representing the overall weekly average. Statistically unusual days are highlighted in red, revealing weekly cycle patterns. Those patterns are often linked to human activity, such as missed observations on weekends or holidays. Automatic stations may also introduce cycles due to maintenance schedules or data recording intervals. These artificial patterns can distort analyses of rainfall frequency, persistence, or seasonality.

- Precision and rounding: A bar plot displays the yearly frequency of decimal digits (0–9), allowing users to detect changes in measurement resolution or rounding patterns over time. Rounding may stem from observer practices (e.g., recording only to the nearest millimeter, tenth of a millimeter, or full integers) or instrumentation constraints. This can distort rainfall intensity distributions, misrepresent light and moderate rainfall events, and introduce long-term biases that affect hydrological modeling and trend detection.

Based on these diagnostics and considering Figure 5, we can easily notice the contrast between the two time series. In the high-quality series (raw_data_00), the precipitation patterns appear continuous and consistent across the entire period with no evident truncation. The small gaps plot shows a good even distribution of light precipitation across different sub-millimeter ranges and years, suggesting minimal omissions. The weekly cycle is practically flat with no anomalous days, and the distribution of decimal frequencies remains balanced over time, indicating stable measurement precision.

On the other hand, the low-quality series (raw_data_01) displays multiple issues. A truncation period is evident (1980 to 1990), where fixed high values (approximately 20 mm) dominate the time series, possibly due to gauge overflow. The small gaps plot reveals years (1970 to 2010) with substantial drops in light precipitation, pointing to systematic underreporting of drizzle or light rain. The weekly cycle is irregular, with Sundays showing a significantly high wet-day fraction, hinting at observer-related biases. Finally, the rounding and precision plot shows an important shift around 1990, indicating changes in instrumentation or data handling practices.

This comparison highlights how enhanced QC tools can uncover subtle but critical issues that would otherwise go unnoticed, supporting more robust data preparation and improving the reliability of downstream analyses. However, when dealing with larger datasets, the visual approach may not be practical. In such cases, automation of the enhanced QC is proposed through the use of a level-criteria definition with the `eqc_Ts()` function.

To illustrate `eqc_Ts()`, we compared two datasets with prior knowledge of their quality: Switzerland and Aragón (Spain). For Switzerland, we used the Swiss NBCN, while for Aragón, precipitation data were collected from public sources (National Meteorological Service of Spain – AEMET) and automatic hydrological monitoring systems.

The quality level distribution for Switzerland and Aragón, displayed in Figure 6, reflects clear differences between the two datasets. In Switzerland, almost all stations were classified as level 0, indicating consistently high data quality. Only a few stations were flagged as level 1, mainly due to minor issues such as truncation effects. In contrast, the Aragón dataset showed a broader spread across levels 0, 1, and 2. Many stations were flagged at level 2, suggesting more frequent issues across all enhanced QC tests, especially small gaps and precision/rounding patterns. The mixture of data sources in Aragón likely contributes to this variability. In general, these results demonstrate how the enhanced QC framework can detect both station-level problems and broader network inconsistencies, helping guide better data selection and preparation for modeling.

While this experiment demonstrates the effectiveness of the enhanced QC framework, it is important to recognize its limitations. The automatic classification can distinguish clear cases of high- or low-quality series but may be less sensitive to intermediate-quality conditions. Moreover, the performance of the enhanced QC can be influenced by the prevailing climate regimes, whether the region is predominantly wet, dry, or transitional, as highlighted by Huerta et al. (2024). Nevertheless, the flexible design, allowing users to adjust level definitions, ensures adaptability across different datasets, climate regimes, and project needs. Beyond its role in supporting reconstruction workflows, the enhanced QC opens up promising opportunities for broader applications, such as the systematic evaluation of citizen weather station networks or quality control in multi-source precipitation datasets. By improving our ability to identify and address data inconsistencies, enhanced QC contributes to building more reliable, inclusive, and resilient climate data infrastructures for future research and decision-making.

4.3. Homogenization

To complement the enhanced quality control, reddPrec introduces a homogenization function designed to detect and adjust hidden inhomogeneities in daily precipitation series. The function implements a multi-test detection strategy combined with a quantile-based adjustment procedure, offering a flexible and automated workflow for improving dataset consistency.

Testing homogenization algorithms on daily precipitation remains particularly challenging. Unlike air temperature data, for which benchmark datasets and well-established evaluation frameworks are available, precipitation series are more variable, discontinuous, and lack widely accepted benchmarks at daily timescales.

To address this gap, we constructed a corrupted version of the Swiss NBCN dataset by introducing controlled random artifacts into the original series. This synthetic corruption adds obvious inhomogeneities, such as shifts in bias, variance, and frequency, while preserving a known ground truth for evaluation. Full details of the corruption procedure are provided in Appendix B. Using this corrupted dataset, we evaluated the reddPrec homogenization module exclusively on the corrupted series (1960-2015), focusing on three main components: break detection, adjustment performance, and trend preservation.

First, break detection performance was assessed using two metrics: Break Detection Accuracy (BDA) and Timing Accuracy (TA). Both metrics range from 0 to 1, where values near 1 indicate more accurate detection (Appendix A). Specifically, a BDA close to 1 means a high proportion of true breaks were correctly identified, while a TA near 1 indicates that all true break points were detected within the specified tolerance window. Second, for adjustment performance, we evaluated how well the method corrected the corrupted precipitation series by computing the mcc and dr metrics, comparing the adjusted series with the original uncorrupted data. Third, for trend preservation, we examined whether the homogenization procedure retained the short-term trends by calculating linear slopes on the PRCPTOT and R1mm indices. The agreement between the original and homogenized trends was assessed using the mcc-slope and dr-slope metrics (mcc and dr applied to slopes).

For this evaluation, we applied the `hmg_Ts()` function with the following settings: `neibs_min = 2`, `neibs_max = 12`, `cor_neibs = 0.5`, `wet_day = -1`, `perc_break = 22`, `apply_qc = 0.5`, and `mm_apply_qc = 0.1`, allowing the method to automatically define adjustment periods. Although setting `wet_day = -1` (including adjustment of zero-precipitation values) is not advisable when working with real datasets, it was adopted here to correct the artificially introduced inhomogeneities in the corrupted series. In operational settings, it is crucial to ensure that real precipitation series undergo thorough quality control and are free from obvious errors before homogenization. The outcomes of the evaluation, including break detection accuracy, adjustment performance, and trend preservation, are summarized in Figure 7.

In the break detection evaluation, the homogenization method demonstrated strong performance in identifying the majority of artificial breakpoints, as indicated by a high BDA value (above 0.7). The TA results further confirmed the method's precision, with detected breakpoints falling within a narrow window around the true dates, supported by the $\pm$1-year tolerance criterion for breakpoint agreement.

Regarding adjustment performance, the method showed notable success in correcting the corrupted series. Both mcc and dr scores improved significantly following homogenization, indicating enhanced agreement with the original uncorrupted precipitation characteristics. In particular, mean mcc and dr values exceeded 0.7, reflecting effective adjustment. However, a higher variance was observed in mcc compared to dr, suggesting greater uncertainty in correcting wet/dry day frequencies than precipitation amounts.

In terms of short-term trend preservation, the method achieved moderate to high success. The linear slopes calculated from the PRCPTOT and R1mm indicators exhibited moderate and high mcc values (around 0.7 and 0.5, respectively), reflecting good agreement in the directionality of trends (i.e., correct identification of positive and negative trends). Meanwhile, moderate dr values (approximately around 0.5) indicated that although the general magnitude of trends was captured, discrepancies remained regarding their exact strength.

Overall, these experiments confirmed that the homogenization procedure is effective not only in detecting and adjusting hidden inhomogeneities but also in retaining the broader precipitation patterns and short-term trends, even in the presence of artificially introduced disturbances.

To further explore the impact of homogenization, we extended the analysis by comparing long-term trend slopes using both the homogenized corrupted data and the real Swiss NBCN data over the full period. Additionally, we applied the homogenization function (using the same parameters as above, except setting `wet_day = 0`) directly to the real dataset to assess potential changes. While the Swiss NBCN dataset is often assumed to be reliable, this exercise allowed us to examine potential inherent inhomogeneities and evaluate whether applying homogenization would reveal significant changes. Results from these comparisons are displayed in Figure 8.

Figure 8a reveals a notable impact on long-term trends after adjusting the corrupted data. Although the corrupted series were effectively corrected overall, the magnitude of the original trends was more difficult to replicate exactly (dr close 0.0). This effect was mainly observed in stations where artificial corruption was introduced (red points), while uncorrupted stations (blue points) remained practically unchanged by the homogenization, as expected (dr and mcc close to 1).

Considering the homogenization of the original Swiss NBCN dataset (Figure 8b), we observed some minor adjustments, with slight changes in long-term trends compared to the original data (dr and mcc close to 1). These effects were more pronounced for the magnitude of PRCPTOT trends than for R1mm trends.

These extended findings highlight the intrinsic difficulty of precisely recovering original long-term trends after correcting local inhomogeneities in daily precipitation series. Even moderate adjustments made to correct breakpoints can introduce noticeable impacts on long-term trends. Nevertheless, the application of homogenization to the real Swiss NBCN dataset confirmed that the method does not introduce major false corrections: stations without significant inhomogeneities remained largely unchanged. This supports the reliability of the homogenization procedure in practice. Further investigation into the homogenization of high-quality networks would be valuable, but this lies beyond the scope of the present study.

In summary, the homogenization approach implemented in reddPrec demonstrates strong potential for detecting and adjusting hidden inhomogeneities in reconstructed daily precipitation series while preserving key precipitation patterns and trends. Nevertheless, some limitations were identified: although the correction of localized breaks was generally effective, the precise reconstruction of long-term trends proved more difficult, highlighting the sensitivity of daily precipitation to small adjustments. It is important to note that this homogenization procedure is specifically designed for reconstructed precipitation datasets, where small inconsistencies are not only from physical measurement errors but may arise from the reconstruction process itself. In this sense, the homogenization of reconstructed precipitation offers an additional "view" of precipitation variability, complementing traditional observations and reconstructions, similar to the framework proposed in Huerta et al. (2024). Thus, reddPrec's homogenization tool contributes a novel perspective to the growing efforts to refine and enhance precipitation datasets for climatic and hydrological studies.

5. Future developments, limitations, and conclusions

In this work, we presented reddPrec as a versatile tool for reconstructing daily precipitation series, featuring advanced quality control, gap-filling, homogenization, and grid creation procedures. The method offered is highly flexible and easy to use. However, future research is needed to incorporate other climate variables (such as air temperature), broadening its scope. Adding uncertainty quantification tools for the enhanced quality control and homogenization would help assess result reliability and strengthen the package. Furthermore, expanding reddPrec to support additional programming languages (Python and Julia) would increase its usability and reach, enabling a broader user base and facilitating integration with various platforms.

In conclusion, reddPrec provides a robust tool for reconstructing precipitation data, offering flexibility for climate research. While challenges remain, the package represents a significant step toward creating high-quality, reproducible precipitation datasets. Continued development will expand its capabilities and make it even more valuable for a diversity of fields.

6. CRediT authorship contribution statement

Adrian Huerta: Writing – original draft, Writing – review & editing, Visualization, Software, Methodology, Investigation, Formal analysis, Data curation, Conceptualization. **Stefan Brönnimann**: Writing – review & editing, Supervision. **Martín de Luis**: Writing – review & editing, Supervision. **Santiago Beguería**: Writing – review & editing, Supervision. **Roberto Serrano-Notivoli**: Writing – review & editing, Visualization, Supervision, Methodology, Conceptualization.

7. Declaration of competing interest

The authors declare that they have no known competing financial interests or personal relationships that could have appeared to influence the work reported in this paper.

8. Software and data availability

The stable version of reddPrec is available on CRAN (`https://doi.org/10.32614/CRAN.package.reddPrec`) and the latest available on GitHub (`https://github.com/rsnotivoli/reddPrec`, last access: 10 Jun 2025). The data and code of the demonstration examples are available at Figshare (Huerta, 2025) and Github (`https://github.com/adrHuerta/examples-reddPrec`, last access: 10 Jun 2025).

9. Acknowledgements

Adrian Huerta acknowledges support from Swiss Government Excellence Scholarships for Foreign Scholars (ESKAS-Nr: 2023.0404). Roberto Serrano-Notivoli is supported by grant RYC2021-034330-I funded by `MCIN/AEI/10.13039/501100011033` and by "European Union NextGenerationEU/PRTR". The authors are grateful for the availability of precipitation data from the National Meteorological Services of Switzerland (MeteoSwiss, `https://www.meteoswiss.admin.ch`) and Spain (AEMET, `https://www.aemet.es/es/portada`). In addition, we acknowledge the EarthEnv topographic (`https://www.earthenv.org/topography`) and MODIS Aqua (`https://doi.org/10.5067/MODIS/MYD09GQ.061`) data products.

References

AEMET, 2024. Informe sobre el episodio meteorolÓgico de precipitaciones torrenciales y persistentes ocasionadas por una dana el dÍa 29 de octubre de 2024. URL: https://www.aemet.es/documentos/es/conocermas/recursos_en_linea/publicaciones_y_estudios/estudios/informe_episodio_dana_29_oct_2024_.pdf. [Accessed 02-05-2025].

Aybar, C., Fernández, C., Huerta, A., Lavado, W., Vega, F., Felipe-Obando, O., 2020. Construction of a high-resolution gridded rainfall dataset for Peru from 1981 to the present day. Hydrological Sciences Journal 65, 770–785.

Begert, M., 2007. Die Überführung der klimatologischen Referenzstationen der Schweiz in das Swiss National Climatological Network (Swiss NBCN). Bundesamt für Meteorologie und Klimatologie, MeteoSchweiz.

Beguería, S., Molina, C.A., Serrano, S.M.V., 2024. Ground records and spatial fields of the 2024/10/29 extreme precipitation event in Valencia, Spain [Dataset]. doi:https://doi.org/10.20350/digitalCSIC/16716.

Bessaklia, H., Serrano-Notivoli, R., Ghenim, A.N., Chikh, H.A., Megnounif, A., 2021. Extreme precipitation trends in northeast Algeria using a high-resolution gridded daily dataset. International Journal of Climatology 41, 6573–6588. URL: https://rmets.onlinelibrary.wiley.com/doi/abs/10.1002/joc.7213, doi:https://doi.org/10.1002/joc.7213, arXiv:https://rmets.onlinelibrary.wiley.com/doi/pdf/10.1002/joc.7213.

Bliefernicht, J., Salack, S., Waongo, M., Annor, T., Laux, P., Kunstmann, H., 2022. Towards a historical precipitation database for West Africa: Overview, quality control and harmonization. International Journal of Climatology 42, 4001–4023.

Brugnara, Y., Good, E., Squintu, A.A., van der Schrier, G., Brönnimann, S., 2019. The EUSTACE global land station daily air temperature dataset. Geoscience Data Journal 6, 189–204. doi:https://doi.org/10.1002/gdj3.81.

Centella-Artola, A., Bezanilla-Morlot, A., Serrano-Notivoli, R., Vázquez-Montenegro, R., Sierra-Lorenzo, M., Chang-Dominguez, D., 2023. A new long term gridded daily precipitation dataset at high-resolution for Cuba (CubaPrec1). Data in Brief 48, 109294. doi:https://doi.org/10.1016/j.dib.2023.109294.

Cheng, V.Y., Wang, X.L., Feng, Y., 2024. A quality control system for historical in situ precipitation data. Atmosphere-Ocean 62, 271–287.

Chicco, D., Jurman, G., 2023. The Matthews correlation coefficient (MCC) should replace the ROC AUC as the standard metric for assessing binary classification. BioData Mining 16, 4. doi:https://doi.org/10.1186/s13040-023-00322-4.

Frei, C., Isotta, F.A., 2019. Ensemble spatial precipitation analysis from rain gauge data: Methodology and application in the European Alps. Journal of Geophysical Research: Atmospheres 124, 5757–5778.

Füllemann, C., Begert, M., Croci-Maspoli, M., Brönnimann, S., 2011. Digitalisieren und Homogenisieren von historischen Klimadaten des Swiss NBCN-Resultate aus DigiHom. MeteoSchweiz .

Hothorn, T., 2024. Cran task view: Machine Learning & Statistical Learning. URL: https://cran.r-project.org/web/views/MachineLearning.html.

Hu, Q., Li, Z., Wang, L., Huang, Y., Wang, Y., Li, L., 2019. Rainfall spatial estimations: A review from spatial interpolation to multi-source data merging. Water 11, 579.

Huerta, A., 2025. Demonstration examples for reddPrec v3.0.0. doi:10.6084/m9.figshare.28771181.

Huerta, A., Serrano-Notivoli, R., Brönnimann, S., 2024. SC-PREC4SA: A serially complete daily precipitation dataset for South America. EarthArXiv .

Hunziker, S., Brönnimann, S., Calle, J., Moreno, I., Andrade, M., Ticona, L., Huerta, A., Lavado-Casimiro, W., 2018. Effects of undetected data quality issues on climatological analyses. Climate of the Past 14, 1–20. doi:10.5194/cp-14-1-2018.

Hunziker, S., Gubler, S., Calle, J., Moreno, I., Andrade, M., Velarde, F., Ticona, L., Carrasco, G., Castellón, Y., Oria, C., Croci-Maspoli, M., Konzelmann, T., Rohrer, M., Brönnimann, S., 2017. Identifying, attributing, and overcoming common data quality issues of manned station observations. International Journal of Climatology 37, 4131–4145. doi:10.1002/joc.5037.

Kossieris, P., Tsoukalas, I., Brocca, L., Mosaffa, H., Makropoulos, C., Anghelea, A., 2024. Precipitation data merging via machine learning: revisiting conceptual and technical aspects. Journal of Hydrology 637, 131424.

Montaño-Caro, J.C., Escolero, O., Morales-Casique, E., Silva-Aguilera, R., Blanco-Gaona, S., Florez-Peñaloza, J.R., 2024. Innovative methodology for estimating Mountain-Front Recharge in data-scarce regions: A case study in Mexico City. Journal of South American Earth Sciences 137, 104835.

Navarro, A., García-Ortega, E., Merino, A., Sánchez, J.L., Tapiador, F.J., 2020. Orographic biases in IMERG precipitation estimates in the Ebro River basin (Spain): The effects of rain gauge density and altitude. Atmospheric Research 244, 105068.

Ochoa-Rodriguez, S., Wang, L.P., Willems, P., Onof, C., 2019. A review of radar-rain gauge data merging methods and their potential for urban hydrological applications. Water Resources Research 55, 6356–6391.

Serrano-Notivoli, R., Beguería, S., Saz, M.Á., Longares, L.A., de Luis, M., 2017a. SPREAD: a high-resolution daily gridded precipitation dataset for Spain–an extreme events frequency and intensity overview. Earth System Science Data 9, 721–738. doi:https://doi.org/10.5194/essd-9-721-2017.

Serrano-Notivoli, R., de Luis, M., Beguería, S., 2017b. An R package for daily precipitation climate series reconstruction. Environmental modelling & software 89, 190–195.

Serrano-Notivoli, R., Saz, M.Á., Longares, L.A., de Luis, M., 2024. SiCLIMA: High-resolution hydroclimate and temperature dataset for Aragón (northeast Spain). Data in Brief 56, 110876.

Serrano-Notivoli, R., Tejedor, E., 2021. From rain to data: A review of the creation of monthly and daily station-based gridded precipitation datasets. WIREs Water 8, e1555. doi:https://doi.org/10.1002/wat2.1555.

da Silva, A.R., Bolonhez, B.F., Pinheiro, H.D., 2024. Homogeneity analysis of daily precipitation series in Paraná State, Southern Brazil. Theoretical and Applied Climatology 155, 8077–8088.

Škrk, N., Serrano-Notivoli, R., Čufar, K., Merela, M., Črepinšek, Z., Kajfež Bogataj, L., de Luis, M., 2021. SLOCLIM: a high-resolution daily gridded precipitation and temperature dataset for Slovenia. Earth System Science Data 13, 3577–3592. doi:https://doi.org/10.5194/essd-13-3577-2021.

Squintu, A.A., van der Schrier, G., Brugnara, Y., Klein Tank, A., 2018. Homogenization of daily ECA&D temperature series. International journal of climatology 39, 1243–1261. doi:https://doi.org/10.1002/joc.5874.

Tang, G., Clark, M.P., Newman, A.J., Wood, A.W., Papalexiou, S.M., Vionnet, V., Whitfield, P.H., 2020. SCDNA: A serially complete precipitation and temperature dataset for North America from 1979 to 2018. Earth System Science Data 12, 2381–2409.

Tang, G., Clark, M.P., Papalexiou, S.M., 2021. SC-Earth: A station-based serially complete Earth dataset from 1950 to 2019. Journal of Climate 34, 6493–6511.

Tang, G., Clark, M.P., Papalexiou, S.M., 2022. EM-Earth: The ensemble meteorological dataset for Planet Earth. Bulletin of the American Meteorological Society 103, E996–E1018.

Tapiador, F.J., Turk, F.J., Petersen, W., Hou, A.Y., García-Ortega, E., Machado, L.A., Angelis, C.F., Salio, P., Kidd, C., Huffman, G.J., et al., 2012. Global precipitation measurement: Methods, datasets and applications. Atmospheric Research 104, 70–97.

Venema, V., Trewin, B., Wang, X., Szentimrey, T., Lakatos, M., Aguilar, E., Auer, I., Guijarro, J., Menne, M., Oria, C., et al., 2020. Guidelines on Homogenization 2020 edition. World Meteorological Organization .

Venema, V.K., Mestre, O., Aguilar, E., Auer, I., Guijarro, J.A., Domonkos, P., Vertacnik, G., Szentimrey, T., Stepanek, P., Zahradnicek, P., et al., 2012. Benchmarking homogenization algorithms for monthly data. Climate of the Past 8, 89–115. doi:https://doi.org/10.5194/cp-8-89-2012.

Vermote, E., Wolfe, R., 2021. MODIS/Aqua surface reflectance daily L2G global 250m SIN grid V061.

Vicente-Serrano, S.M., Beguería, S., López-Moreno, J.I., García-Vera, M.A., Stepanek, P., 2010. A complete daily precipitation database for northeast Spain: reconstruction, quality control, and homogeneity. International Journal of Climatology 30, 1146–1163. doi:https://doi.org/10.1002/joc.1850.

Willmott, C.J., Robeson, S.M., Matsuura, K., 2012. A refined index of model performance. International Journal of climatology 32, 2088–2094. doi:https://doi.org/10.1002/joc.2419.

Figures

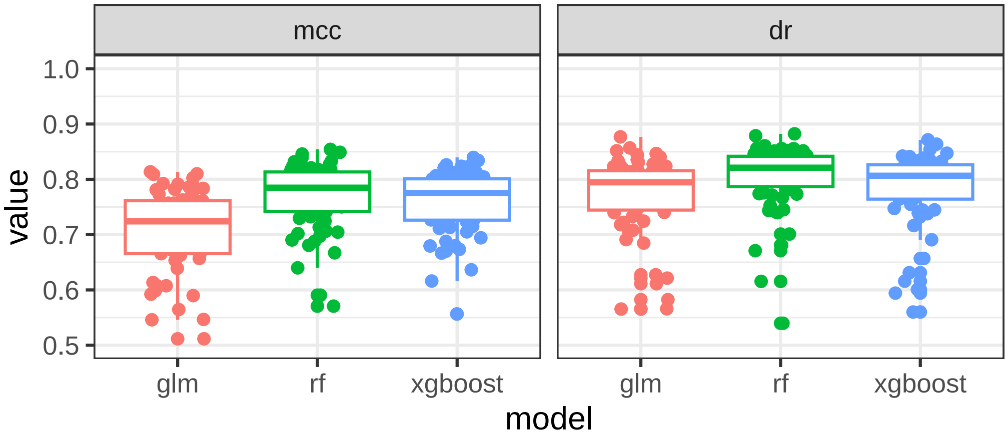

Figure 1: Boxplots of gap-filling evaluation metrics (mcc: Matthews correlation coefficient, dr: refined index of agreement) for precipitation data in Switzerland (2010–2015) from 69 stations. The performance of three gap-filling methods—linear model (glm), random forest (rf), and extreme gradient boosting (xgboost)—is compared based on these metrics. In both plots, the maximum value is one, meaning perfect prediction.

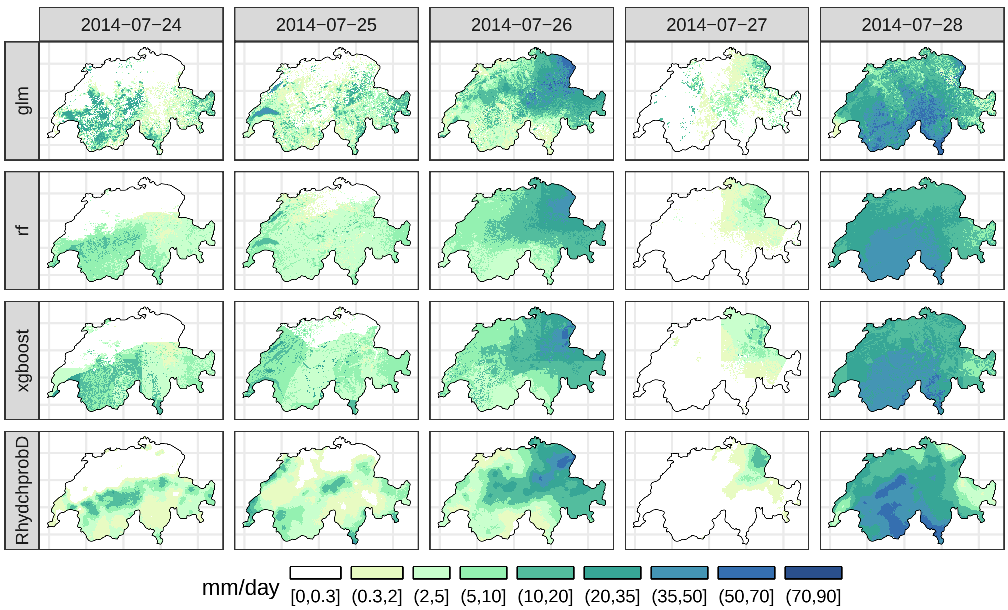

Figure 2: Daily precipitation fields (0.009° ≈ 1 km) for an extreme precipitation event (July 24–28, 2014) in Switzerland. The comparison includes three gridding methods—generalized linear model (glm), random forest (rf), and extreme gradient boosting (xgboost)—along with the median value of the RhydchprobD product. The glm, rf, and xgboost grids were constructed using 69 stations.

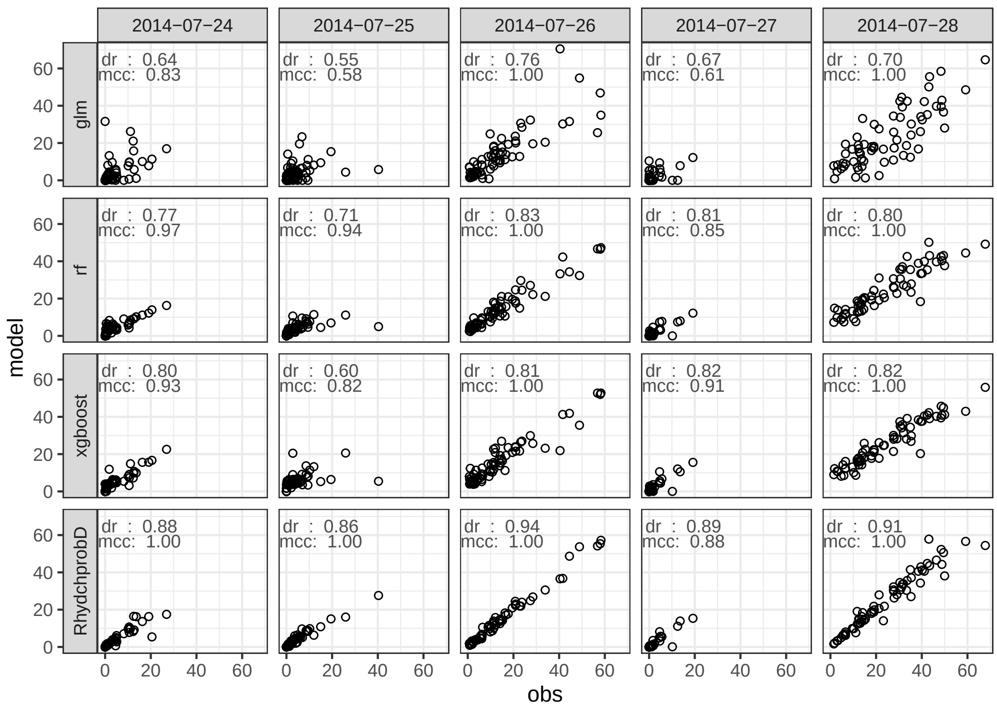

Figure 3: A scatterplot comparing station values with the nearest grid for an extreme precipitation event (July 24–28, 2014) in Switzerland. Each plot displays the evaluation metrics (mcc: Matthews correlation coefficient, dr: refined index of agreement).

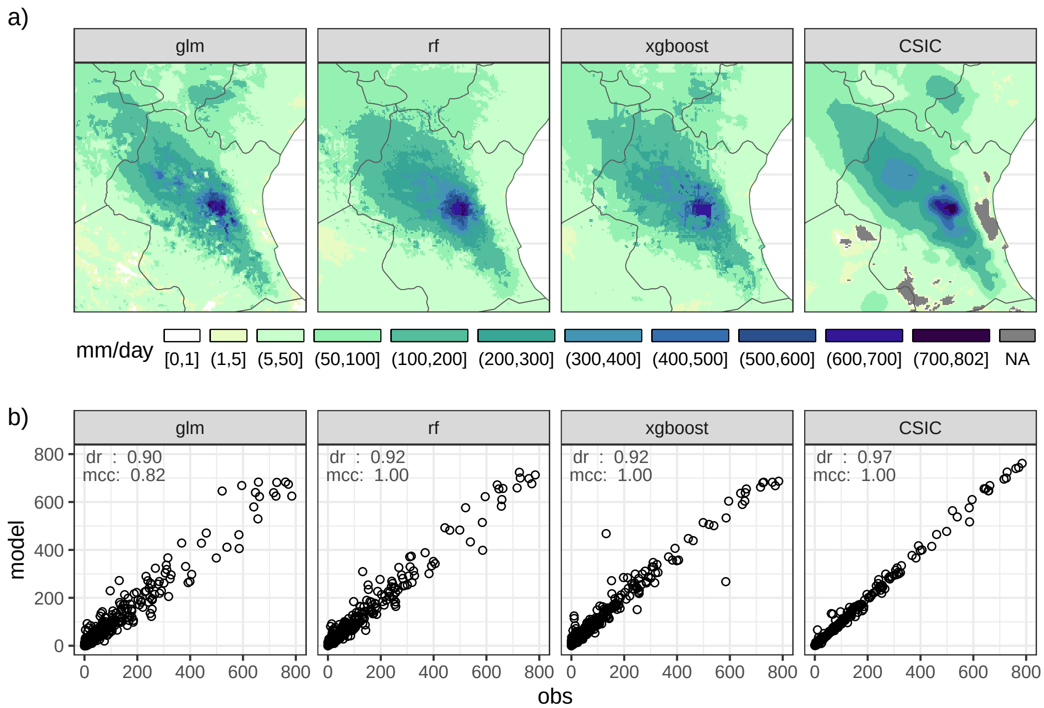

Figure 4: (a) Daily precipitation fields ($0.009^\circ \approx 1$ km) for an extreme precipitation event (October 29, 2024) in Valencia, Spain. (b) A scatterplot comparing station values with the nearest grid values with evaluation metrics (mcc: Matthews correlation coefficient, dr: refined index of agreement) is displayed for each plot. The comparison includes three gridding methods—generalized linear model (glm), random forest (rf), and extreme gradient boosting (xgboost)—along with fields developed by the Consejo Superior de Investigaciones Científicas (CSIC). The glm, rf, and xgboost grids were constructed using data from 443 stations.

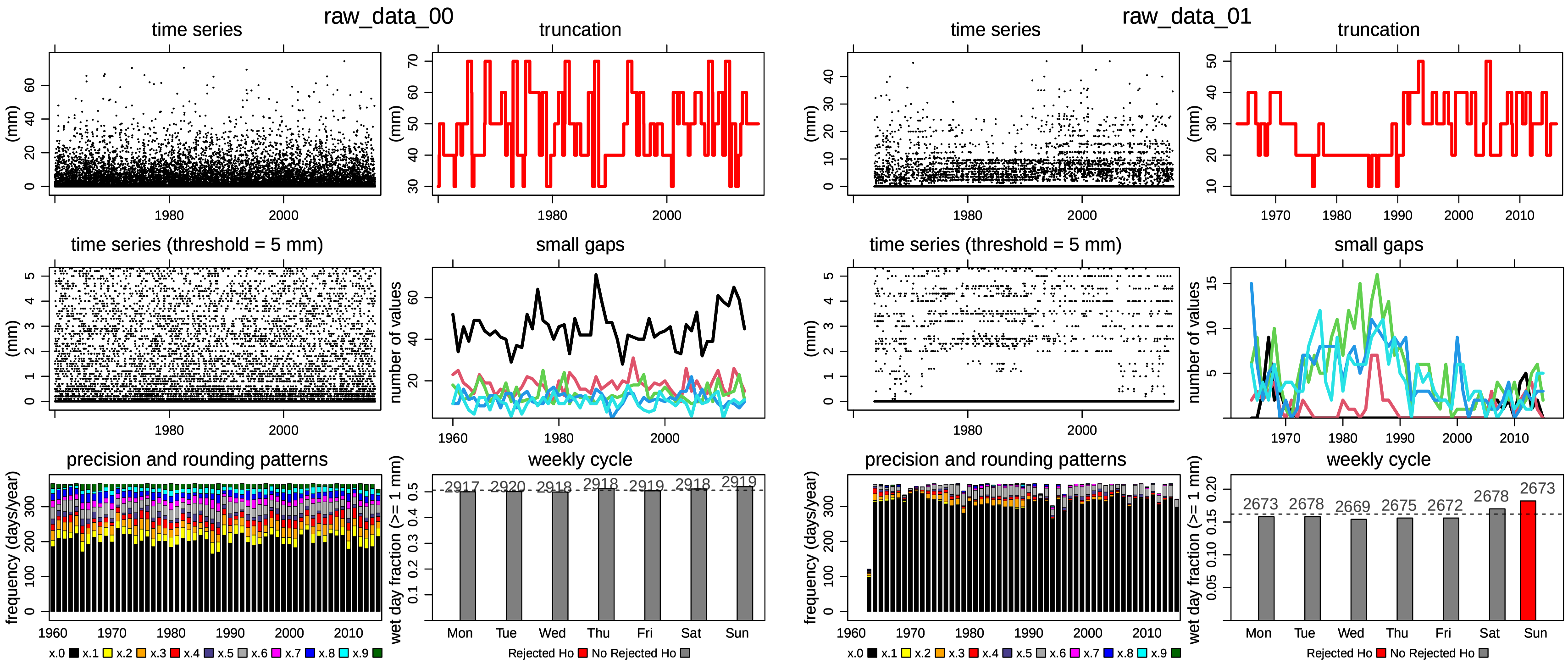

Figure 5: Example enhanced quality control plots for two time series: one from a high-quality station (raw_data_00) and one from a low-quality station (raw_data_01). In addition to the raw time series (including one with a lower precipitation range), the plots illustrate key diagnostic tests applied during quality control—truncation, small gaps, weekly cycle, and precision and rounding patterns.

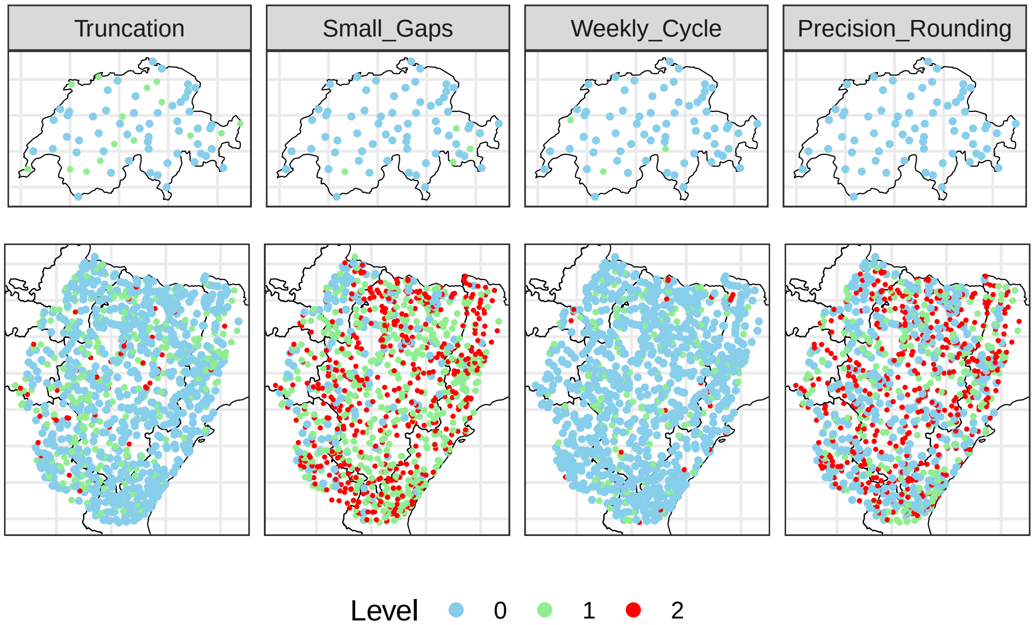

Figure 6: Application of automatic enhanced quality control to daily precipitation data for Switzerland (top) and Aragon (Spain, bottom) during 1980–2015. Each quality control test—truncation, small gaps, weekly cycles, and precision or rounding patterns—displays the assigned quality level (0, 1, or 2) for each station.

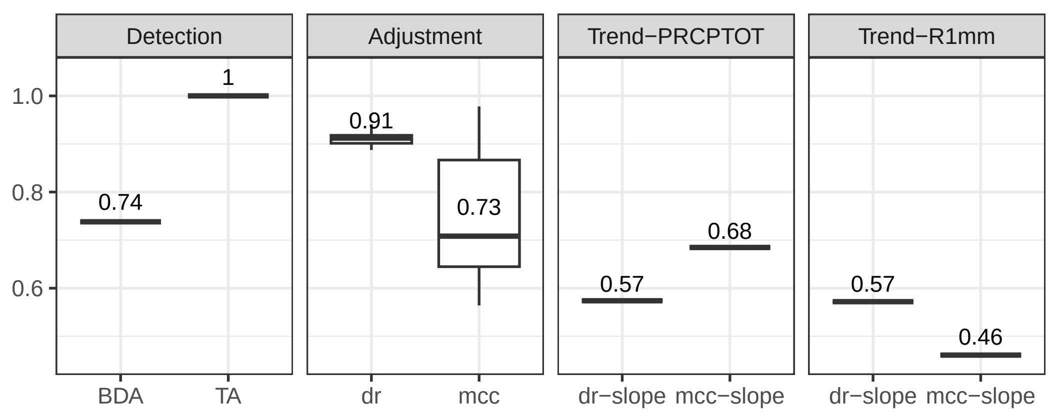

Figure 7: Summary plot for homogenization evaluation between corrupted and original Swiss NBCN: detection (BDA: break detection; and TA: Timing Accuracy), adjustment (dr: refined index of agreement; and mcc: Matthews correlation coefficient), and trend preservation in PRCPTOT and R1mm indices.

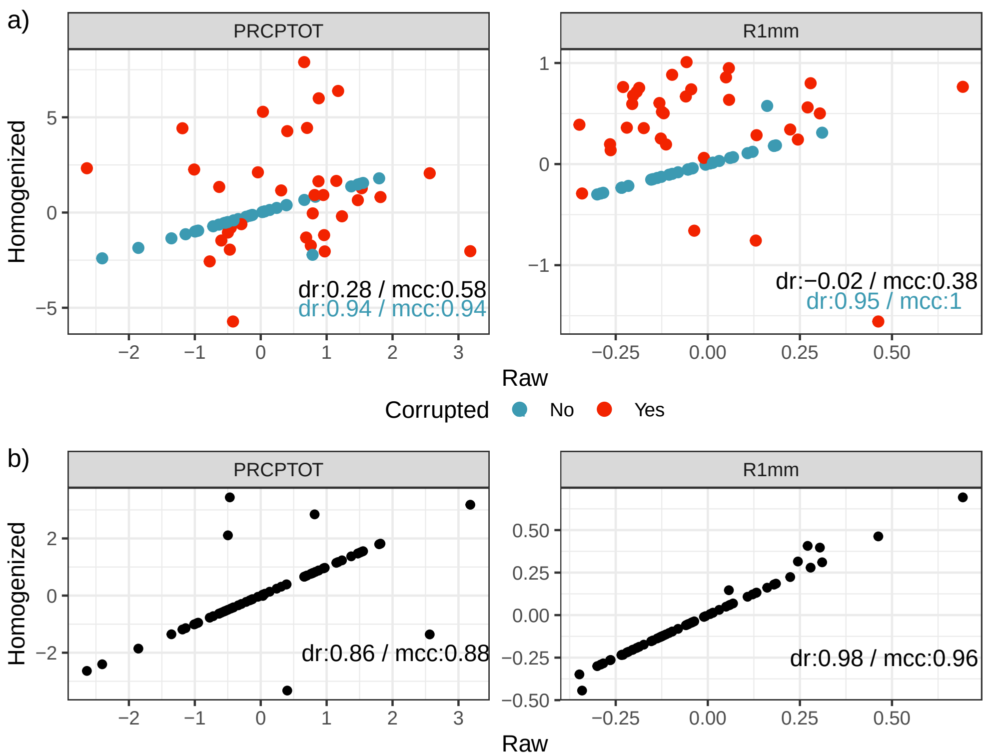

Figure 8: Scatterplot of homogenized and raw trend slopes for PRCPTOT and R1mm indices for the 1960-2015 period. (a) Display the long-term trend slopes between the homogenized corrupted and raw Swiss NBCN. (b) Display long-term trend slopes between the homogenized and raw Swiss NBCN. In the plot, the refined index of agreement (dr) and Matthews correlation coefficient (mcc) metrics are shown. In (a), dr and mcc are computed from the whole sample of points (black) and non-corrupted time series (red).

Appendix A. Metrics used for evaluation

To evaluate the performance of precipitation in the gap-filling and grid creation experiments, we employed two metrics:

- The Matthews correlation coefficient (mcc) is a balanced classification performance measure, particularly suitable for binary classification with imbalanced classes (Chicco and Jurman, 2023). The mcc values range from -1 (total disagreement) to +1 (perfect agreement), with 0 indicating no better than random classification. The mcc is calculated as:

$$mcc = \frac{TP \times TN - FP \times FN}{\sqrt{(TP + FP)(TP + FN)(TN + FP)(TN + FN)}}$$

  where TP denotes the number of days correctly classified as wet (≥ 0.1 mm), TN as days correctly classified as dry (< 0.1 mm), FP as days incorrectly classified as wet, and FN as days incorrectly classified as dry.

- The refined index of agreement (dr) is a modified version of the traditional index of agreement proposed by Willmott et al. (2012). It is suited for continuous variables and aims to improve sensitivity to systematic biases and error distributions. The dr metric ranges from -1 (no agreement) to +1 (perfect agreement), with 0 indicating no predictive skill. The dr is calculated as:

$$dr = 1 - \frac{\sum_{i=1}^{n} |p_i - \hat{y}_i|}{2\sum_{i=1}^{n} |\hat{y}_i - \bar{y}|)}$$

  where n is the number of observations, p_i is the predicted precipitation on day i, $\hat{y}_i$ is the observed precipitation on day i, and $\bar{y}$ is the mean of $\hat{y}_i$.

In addition, for the homogenization experiment, we used two custom metrics:

- The break detection accuracy (BDA) measures the overall accuracy of break detection. The metric ranges from 0 to 1, with higher values indicating more accurate break detection. It's calculated as:

$$BDA = \frac{TP}{TP + FP + FN}$$

  where TP represents the detected breaks that correspond to the true break years, FP the detected breaks that do not correspond to any true break, and FN the true breaks that were missed.

- The timing accuracy (TA) metric measures the temporal precision of break detection. It calculates the proportion of true breaks that were detected within a tolerance (here equal to ± 2 years). TA varies from 0 to 1. A value of 1 indicates that all true breakpoints were detected within the tolerance window, while values close to 0 suggest poor timing between detected and true breakpoints. It is defined as follows:

$$TA = \frac{\text{Number of true breaks detected within tolarence}}{\text{Total number of true breaks}}$$

Appendix B. Construction of corrupted Swiss NBCN.

To test the homogenization approach implemented in reddPrec, we created a synthetically corrupted version of the Swiss NBCN(1960-2015). The original dataset was subjected to random artificial break injections affecting 50% of the stations within the 1970-2000 period.

Three types of artificial changes were introduced:

- Bias shifts: a constant offset (± 2 mm) applied to a portion of the series.
- Variance changes: multiplicative variability alterations ($\times 1.5$).
- Frequency changes: increased wet-day frequency, where selected dry days (0 mm) were converted to wet days using gamma-distributed values.

To ensure consistency with the correction strategy in the demonstration example, only dry-to-wet frequency changes were introduced. The homogenization method relies on the `wet_day` argument to determine whether 0 mm values (dry days) are included in the adjustment process. In this study, `wet_day = 0` was used, meaning dry days were treated as valid values and included in the adjustment, allowing effective correction of added wet-day noise. By contrast, if `wet_day = 1` had been used, zeros would have been excluded from the adjustment procedure, complicating the correction of artificially added dry days. For this reason, wet-to-dry changes were excluded from the corruption setup to maintain coherence with the correction strategy.

The break metadata (station, break date, break years, type of break) were recorded to allow precise evaluation of detection accuracy, adjustment effectiveness, and trend preservation.

Appendix C. Supplementary Figures

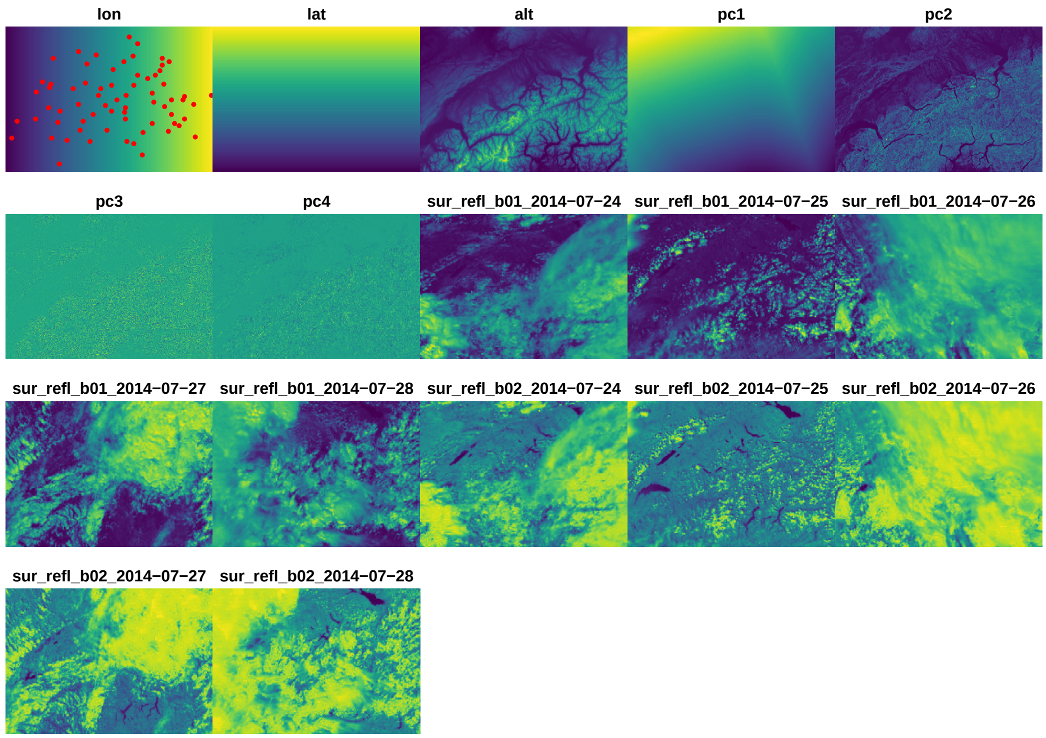

Figure C.9: Spatial covariates for an extreme precipitation event (July 24–28, 2014) in Switzerland. Static covariates include longitude (lon), latitude (lat), elevation (alt), and the first four principal components of topographical covariates (pc1, pc2, pc3, and pc4). Dynamic covariates include surface reflectance (sur_refl) for bands 1 (b01) and 2 (b02). In the first subplot, the stations used for spatial modeling are shown as red dots. Colorbar legends were omitted.

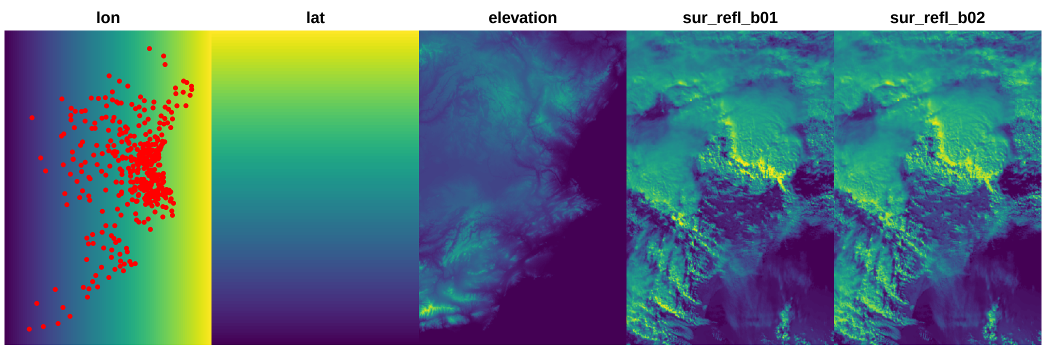

Figure C.10: Spatial covariates for an extreme precipitation event (October 29, 2024) in Valencia, Spain. Static covariates include longitude (lon), latitude (lat), elevation (elevation), and surface reflectance (sur_refl) for bands 1 (b01) and 2 (b02). In the first subplot, the stations used for spatial modeling are shown as red dots. Colorbar legends were omitted.